European Journal of Radiology 115 (2019) 39–45

Contents lists available at ScienceDirect

European Journal of Radiology

journal homepage: www.elsevier.com/locate/ejrad

Preliminary utilization of radiomics in differentiating uterine sarcoma from atypical leiomyoma: Comparison on diagnostic efficacy of MRI features and radiomic features

Huihui Xie[a], Juan Hu[b], Xiaodong Zhang[a], Shuai Ma[a], Yi Liu[a], Xiaoying Wang[a,*]

[a] Department of Radiology, Peking University First Hospital, Beijing, China
[b] Department of Radiology, The First Affiliated Hospital of Kunming Medical University, Kunming, China

ARTICLE INFO

Keywords:
Magnetic resonance imaging
Leiomyoma
Sarcoma
Uterus
Radiomics

ABSTRACT

Objectives: To explore whether MRI and radiomic features can differentiate uterine sarcoma from atypical leiomyoma. And to compare diagnostic performance of radiomic model with radiologists.

Methods: 78 patients (29 sarcomas, 49 leiomyomas) imaged with pelvic MRI prior to surgery were included in this retrospective study. Certain clinical and MRI features were evaluated for one lesion per patient. Radiological diagnosis was made based on MRI features. A radiomic model using automated texture analysis based on ADC maps was built to predict pathological results. The association between MRI features and pathological results was determined by multivariable logistic regression after controlling for other variables in univariate analyses with $P < 0.05$. The diagnostic efficacy of radiologists and radiomic model were compared by area under the receiver-operating characteristic curve (AUC), sensitivity, specificity and accuracy.

Results: In univariate analyses, patient's age, menopausal state, intratumor hemorrhage, tumor margin and uterine endometrial cavity were associated with pathological results, $P < 0.05$. Patient's age, tumor margin and uterine endometrial cavity remained significant in a multivariable model, $P < 0.05$. Diagnosis efficacy of radiologists based on MRI reached an AUC of 0.752, sensitivity of 58.6%, specificity of 91.8%, and accuracy of 79.5%. The optimal radiomic model reached an AUC of 0.830, sensitivity of 76.0%, average specificity of 73.2%, and accuracy of 73.9%.

Conclusions: Ill-defined tumor margin and interrupted uterine endometrial cavity of older women were predictors of uterine sarcoma. Radiomic analysis was feasible. Optimal radiomic model showed comparable diagnostic efficacy with experienced radiologists.

1. Introduction

Uterine sarcomas are heterogenous neoplasms that consists of multiple histopathologic subtypes that associated with a poor prognosis when compared with gynecological carcinoma [1–3]. They are characterized by its aggressive behavior, with a great tendency to local recurrence, early dissemination, distant spread, and high mortality rate [4,5]. Preoperative diagnosis of uterine sarcomas become increasingly important because of the rapidly growing availability of more conservative approaches in the management of benign uterine masses [6]. While those techniques offer benefit of faster recovery and organ-preservation, they could allow uterine sarcoma go unrecognized. Sometimes what presumed to be leiomyomas are subsequently found to be sarcomas [3,7].

The clinical differentiation of uterine sarcoma from leiomyoma is often difficult due to similar symptoms and laboratory data they produce [8,9]. What's more, there are no pathognomonic feature to diagnose uterine sarcoma on any imaging technique [5]. Magnetic resonance imaging (MRI) is able to offer more detailed analysis than CT or ultrasonography in the preoperative diagnosis of uterine sarcoma [9]. Previous studies shown that a solitary, lobulated uterine mass with ill-defined margin, flow voids, intratumor hemorrhage, and intratumor necrosis in MR images of elderly woman raised suspicion of sarcoma [5,8–11]. Tumors located mainly in the uterine cavity also raise suspicion of malignancy [12]. However, due to degeneration, or unusual pattern of growth, atypical leiomyoma may present with similar MRI features [8]. Different results from previous studies have also led to uncertainty regarding the value of MRI features [5,10,13–15].

* Corresponding author at: Department of Radiology, Peking University First Hospital, No. 8, Xishiku Street, Xicheng District, 100034, Beijing, China.
E-mail addresses: xiehuihui1030@163.com (H. Xie), 13619644022@163.com (J. Hu), zhxd2009@gmail.com (X. Zhang), mashuai316@126.com (S. Ma), 993537544@qq.com (Y. Liu), cjr.wangxiaoying@vip.163.com (X. Wang).

https://doi.org/10.1016/j.ejrad.2019.04.004
Received 25 October 2018; Accepted 4 April 2019
0720-048X/

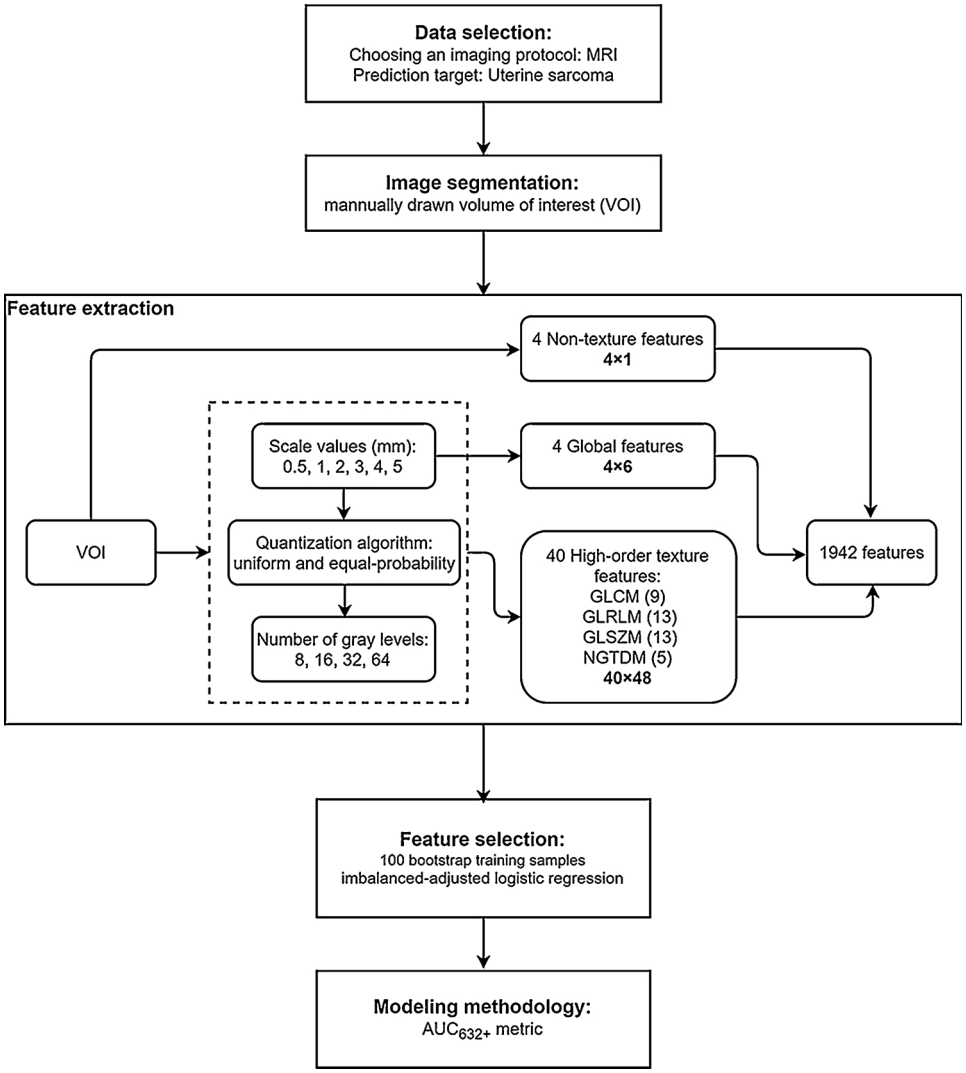

Fig. 1. Workflow of radiomic analysis: (a) data selection; (b) image segmentation; (c) feature extraction; (d) feature selection; and (e) modeling methodology.

Therefore, further investigations are needed.

Radiomics involves extraction and modeling of a large number of medical imaging features for diagnostic, prognostic, and predictive purpose [16,17]. Multiple studies have showed the feasibility of radiomics across imaging modalities in oncology and its effectiveness [18–22]. Lakhman et al. had investigated that texture analysis of T2-weighted images was feasible in distinguished leiomyosarcoma from atypical leiomyoma [8]. However, none of previous studies had investigated whether functional MRI radiomic features could render better prediction of uterine sarcomas.

The purpose of this study is to investigate the whether MR features and apparent diffusion coefficient (ADC) map-based radiomic features can distinguish uterine sarcoma from atypical leiomyoma and to compare the diagnostic efficacy between radiologists and radiomic model.

2. Materials and methods

2.1. Study population

The institutional review board approved this retrospective study with a waiver of the requirement for patients' informed consent. A database of gynecologic surgeries (hysterectomy or myomectomy) performed was reviewed. Consecutive patients were retrieved according to the following inclusion criteria: patients who (a) had histologically proven uterine sarcoma or leiomyoma; (b) were suspected of malignant uterine mass or atypical leiomyoma in their MRI reports or diagnosis on admission; (c) underwent preoperative multiparametric MRI (MP-MRI); (d) had no chemotherapy, radiation or invasive therapy before MP-MRI; and (e) with available clinical information. Pathological diagnosis were made based on the Stanford criteria, supplemented by the World Health Organization's Classification of Tumors of Female Reproductive Organs [23].

2.2. MR imaging acquisition

Patients underwent MRI examinations using either a 3-T system (Achieva; Philips Healthcare, Best, The Netherlands) or a 1.5-T system (Signa HDxt, GE Medical System) in this study. The imaging protocol included: (1) T2-weighted fast spin-echo imaging in the axial, coronal, and sagittal planes; (2) axial T1-weightedd fast spin-echo imaging; (3) axial Diffusion-weighted MRI (DWI) with reconstruction of ADC maps; and (4) dynamic contrast enhanced (DCE) MRI. The parameters are presented in Supplementary Data.

2.3. Assessment of MRI features

One of the authors reviewed MR images and pathologic diagnosis of all included patients. For patients with more than one lesion, this author correlated MR images with relevant pathologic findings and marked one index lesion for further assessment. Another two

Table 1
Pathological diagnosis.

Pathological results	Uterine sarcoma Frequency (%)	Uterine leiomyoma Frequency (%)
Uterine sarcoma (N = 29)		
Mesenchymal sarcoma	19/29 (65.5)	
Leiomyosarcoma	10/29 (34.5)	
Endometrial stromal sarcoma	5/29 (17.2)	
Rhabdomyosarcoma	1/29 (3.4)	
Undifferentiated uterine sarcoma	3/29 (10.3)	
Mixed epithelial and mesenchymal sarcoma	10/29 (34.5)	
Carcinosarcoma	7/29 (24.1)	
Adenosarcoma	3/29 (10.3)	
Uterine leiomyoma (N = 49)		
Leiomyomas		41/49 (83.7)
Red degeneration		2/41 (4.9)
Hyaline degeneration		20/41 (48.8)
Hydropic degeneration		1/41 (2.4)
Without specific degeneration		18/41 (43.9)
Cellular leiomyomas		8/49 (16.3)

radiologists (with 5-years and 21-year experience in genitourinary imaging), both blinded to the pathologic diagnosis and clinical information, were asked to evaluate several MRI features and reach a radiologic diagnosis (sarcoma or leiomyoma) for each index lesion. MRI features included: (a) the maximal diameter of index lesion; (b) tumor margin (well-defined or ill-defined) on T2WI; (c) tumor shape (smooth or lobulated) on T2WI; (d) flow void on T2WI (absent or present); (e) intratumor hemorrhage (defined as hyperintensity on T1WI, recorded as absent or present); (f) necrosis or cystic change (defined as hypointensity on T1WI, hyperintensity on T2WI, and unenhanced areas on DCE, recorded as absent or present); (g) uterine endometrial cavity (defined as continuous or discontinuous hyperintensity of uterine endometrial cavity on T2WI, recorded as uninterrupted or interrupted). During the image interpretation, interobserver disagreement was discussed until consensus was reached, if consensus cannot be reached, final disagreement was solved in a panel format including one additional coauthor. In the end, binary radiologic diagnosis was reached for each patient in consensus.

2.4. Radiomics analysis

In 2015, Vallières et al. [24] first introduced a radiomics model built from joint PET and MRI texture features using bootstrapping evaluations. In 2017 and 2018, Zhou et al. [25] and Dong et al. [26] adopted this method in predicting survival and molecular markers in diffuse lower-grade gliomas and sentinel lymph node metastasis in breast cancer with high sensitivity and specificity. In this study, similar methods were used for radiomic analysis in this study.

Radiomic analysis contains five major steps: data selection, image segmentation, feature extraction, feature selection and modeling (Fig. 1). Segmentation of images into volume of interest (VOI) which covered the index lesion was performed using MRIcron (version 1.40) by a junior radiologist and supervised by a senior radiologist. Each VOI was manually drawn slice-by-slice on ADC maps with reference to T2WI and DWI. 4 non-texture features and 43 texture features were extracted from each VOI using combinations of following extraction parameters: (1) 3D isotropic scales of 0.5 mm, 1 mm, 2 mm, 3 mm, 4 mm, and 5 mm; (2) “uniform” and “equal-probability” quantization algorithm; (3) number of gray levels of 8, 16, 32, and 64. Initial feature sets selection was achieved using 100 bootstrap training samples to yield reduced feature set of 50 different features. Then, feature selection was performed by maximizing 0.632+ area under the receiver-operating characteristic curve (AUC) metric to obtain texture models combining 1–20 variables (model order). Multivariate models were constructed for each initial feature set and modeled binary outcome using imbalanced-adjusted logistic regression. To demonstrate the predictive performance of the optimal model, final logistic regression coefficients were computed using 100 bootstrap training samples. The probability of uterine sarcoma as a function of the response of optimal multivariable model was calculated in the bootstrap samples [25].

2.5. Statistical analysis

Software (SPSS, version 23.0; SPSS, Chicago, III) was used for statistical analysis. Continuous data were summarized with means and ranges; categorical variables were described with frequencies and percentages. Mann-Whitney U test, independent t test, Chi-square test and Fisher exact test were used as appropriate for the univariate analysis. A P value of < 0.05 was considered statistically significant. Multivariable logic regression was used to determine factors that were independently associated with pathological result. Before consensus were reached, the interobserver agreement for the MRI features was assessed using the kappa consistency test. Kappa values > 0.81, in the range of 0.61 and 0.80, and < 0.60 were considered to reflect excellent, good, and poor agreement, respectively. The diagnostic efficacy of radiologists and radiomic model were compared by AUC, sensitivity, specificity and accuracy.

3. Results

3.1. Study population

The distribution of the pathological results is summarized in Table 1. Between July 2010 and November 2016, 29 patients with uterine sarcoma and 49 patients with atypical leiomyoma who complied with the inclusion criteria were included in this study.

The clinical data of the patients are listed in Table 2. Patients with uterine sarcomas were significantly older than those who had leiomyomas ($P < 0.0001$). Leiomyomas (91.8%) were more frequently found in women during premenopausal stage while more patients with sarcomas (75.9%) were post-menopausal ($P < 0.000001$). The most common symptoms leading to MRI examinations were abnormal vaginal bleeding for patients with uterine sarcoma (58.6%) and menstrual changes for patients with uterine leiomyoma (36.7%). 28.6% patients with atypical leiomyoma had no symptoms while all patients with sarcoma were not symptom-free. This difference was obviously significant ($P = 0.01$). The maxim diameters of index lesion of the two groups had no significant difference ($P = 0.525$).

Table 2
Clinical characteristics.

	Uterine sarcoma Mean or frequency (Range or %)	Uterine leiomyoma Mean or frequency (Range or %)	P value
Age (years)	58.7 (38~77)	38.8 (23~60)	< **0.0001**
Menopausal state			
Premenopausal	7/29 (24.1)	45/49 (91.8)	< **0.000001**
Postmenopausal	22/29 (75.9)	4/49 (8.2)	
Clinical manifestation			
Abnormal vaginal bleeding	17/29 (58.6)	7/49 (14.3)	< **0.0001**
Menstrual changes	3/29 (10.3)	18/49 (36.7)	**0.016**
Abdominal pain	5/29 (17.2)	3/49 (6.1)	0.14
Pelvic mass	6/29 (20.7)	7/49 (14.3)	0.536
Physical examination	0	14/49 (28.6)	**0.001**
Maximal diameter of index lesion (cm)	7.5 (1.5~18.7)	6.7 (2.0~12.4)	0.525

Table 3
Interobserver agreements on qualitative MRI features.

	Kappa value (Uterine sarcoma)	Kappa value (Uterine leiomyoma)
Tumor Margin	0.631	1
Tumor Shape	0.861	0.672
Flow voids	0.725	0.712
Intratumor hemorrhage	0.654	0.878
Necrosis or cystic change	0.731	0.778
Uterine endometrial cavity	0.931	0.79

Table 4
Qualitative MRI features.

	Uterine sarcoma (N = 29) Frequency (%)	Uterine leiomyoma (N = 49) Frequency (%)	P value
Tumor Margin			
Well-defined	20/29 (69.0)	49/49 (100)	< **0.0001**
Ill-defined	9/29 (31.0)	0/49 (0)	
Tumor Shape			
Smooth	15/29 (51.7)	31/49 (63.3)	0.3488
Lobulated	14/29 (48.3)	18/49 (36.7)	
Flow voids			
Absent	13/29 (44.8)	27/49 (55.1)	0.4831
Present	16/29 (55.2)	22/49 (44.9)	
Intratumor hemorrhage			
Absent	15/29 (51.7)	44/49 (89.8)	**0.0002**
Present	14/29 (48.3)	5/49 (10.2)	
Necrosis or cystic change			
Absent	7/29 (24.1)	18/49 (36.7)	0.3187
Present	22/29 (75.9)	31/49 (63.3)	
Uterine endometrial cavity			
Interrupted	16/29 (55.2)	2/49 (4.1)	< **0.0001**
Uninterrupted	13/29 (44.8)	47/49 (95.9)	

3.2. Assessment of MRI features

Interobserver agreement levels regarding MRI features were good to excellent (kappa value = 0.654 ~ 1.000) (Table 3). The qualitative MRI features of the two groups are summarized in Table 4. 20 (69%) uterine sarcomas had ill-defined tumor margin on T2WI while all leiomyomas had well-defined margins ($P <$ 0.0001). 14 (48.3%) patients with uterine sarcoma were presented with intratumor hemorrhage on T1WI while only 5 (10.2%) patients with leiomyoma had intratumor hemorrhage ($P =$ 0.0002). 16 (55.2%) patients with uterine sarcoma and 2 (4.1%) patients with leiomyoma had interrupted uterine endometrial cavity on T2WI ($P <$ 0.0001). There was no significant difference in the tumor shape, intratumor necrosis or cystic change, and peri- or intratumor flow voids between the two groups (P values were 0.3488, 0.3187, and 0.4831, respectively). Fig. 2 shows an example of different MRI features. Multivariable logistic regression identified that older age, ill-defined tumor margin and interrupted uterine endometrial cavity were significant preoperative predictive factors for uterine sarcoma. (P values were 0.000, 0.000 and 0.001, respectively). In 49 patients with uterine leiomyoma. 4 patients were mistakenly diagnosed as uterine sarcoma. In 29 patients with uterine sarcoma, 12 patients were mistakenly diagnosed as uterine leiomyoma. Diagnosis efficacy of radiologists reached an AUC of 0.752, sensitivity of 58.6%, specificity of 91.8%, and accuracy of 79.5%.

3.3. Radiomic analysis

Feature set reduction and feature selection using imbalanced-adjusted logistic regression and bootstrap resampling, texture models with orders 1–20 that maximized the AUC metric were computed for the feature sets extracted from VOIs to model the binary outcomes (leiomyoma or sarcoma) (Fig. 3). Model 18 with 18 features yielded the highest AUC of 0.830, sensitivity of 76.0%, average specificity of 73.2%, and accuracy of 73.9%. The optimal feature set included 13 high-order texture features (Entropy, Contrast, Correlation, Homogeneity, Energy, Variance, Dissimilarity, Complexity, Gray-Level Non-uniformity, and Zone-Size Non-uniformity) and 2 histogram-based texture features (Variance and Kurtosis).

The probability of observing uterine sarcoma as a function of the response of the multivariable models proposed in this work was calculated for all patients of the cohort (Fig. 4). The probability 1 suggests uterine sarcoma, 0 suggests uterine leiomyoma with a threshold of 0.5. In 29 patients with uterine sarcoma, probability of only 1 patient was under 0.5. In 49 patients with uterine leiomyoma, probabilities of 6 patients were above 0.5.

4. Discussion

To differentiate uterine sarcoma from atypical leiomyoma is a clinical challenge [8]. In this study, we investigated whether certain clinical and MRI features can help distinguishing uterine sarcoma from atypical leiomyoma. We also investigated whether machine learning method can be adopted in this difficult task and compared its predictive performance with radiologists.

First, this study demonstrated that older age, postmenopausal state, abnormal vaginal bleeding, ill-defined tumor margin, intratumor hemorrhage, and interrupted uterine endometrial cavity were strong predictors for uterine sarcoma. Patient's age, tumor margin and uterine endometrial cavity remained significant in a multivariable model. These clinical and MRI predictors are easily accessible for radiologists and clinicians.

In this study, most patients with uterine sarcomas were in the fifth and sixth decade of age and lots of them were postmenopausal, while patients with uterine leiomyoma were younger, which was similar with previous studies [8–10]. Rapid mass enlargement after menopause may signify malignancy [27]. It may also be observed with cellular or degenerating leiomyoma [28]. However, in our study, the rate of tumor growth was not possible for most large masses were discovered at the initial encounter. The maximal diameter of index lesion at presentation showed no difference in our groups. Intratumor unenhanced area were not reliable because degenerations were very common in uterine leiomyomas, especially in large and atypical ones [27]. Increased vascularity around or inside the tumor was not reliable, either, which contrast to previous studies [5,8,9]. Intratumor hemorrhage, indistinct borderline of tumor, and interrupted uterine endometrial cavity had statistical associations with uterine sarcomas, which were similar to previous studies [5,8,10–12].

Second, radiomics has been proved to characterizes intratumor heterogeneity to improve cancer diagnosis, prognosis, and prediction of response to treatment [18–22]. In this research, we demonstrated that radiomic features can differentiate uterine sarcoma from atypical leiomyoma in a non-invasive method. These radiomic features were extracted from routinely acquired MR images. Lakhman et al. had investigated texture features extracted from T2WI to differentiate leiomyosarcoma from atypical leiomyoma and concluded that leiomyosarcoma had greater heterogeneity [8]. This study stood out from previous radiomic studies because was the first one to do radiomic analysis on ADC maps to predict uterine sarcoma. DWI has been proposed as a tumor imaging biomarker and the ADC value determined by DWI varies inversely with tissue cellularity [29,30]. ADC maps were used for radiomic analysis because DWI sequence of different MR scanners may vary in b values. Dozens of studies in vivo have shown that Several studies have investigated the utility of DWI and ADC maps in the diagnosis of gynecological malignancies [14,15,31]. According to our result, textural features (Global, GLCM, GLRLM, GLSZM and NGTDM) extracted from ADC maps are correlated with uterine

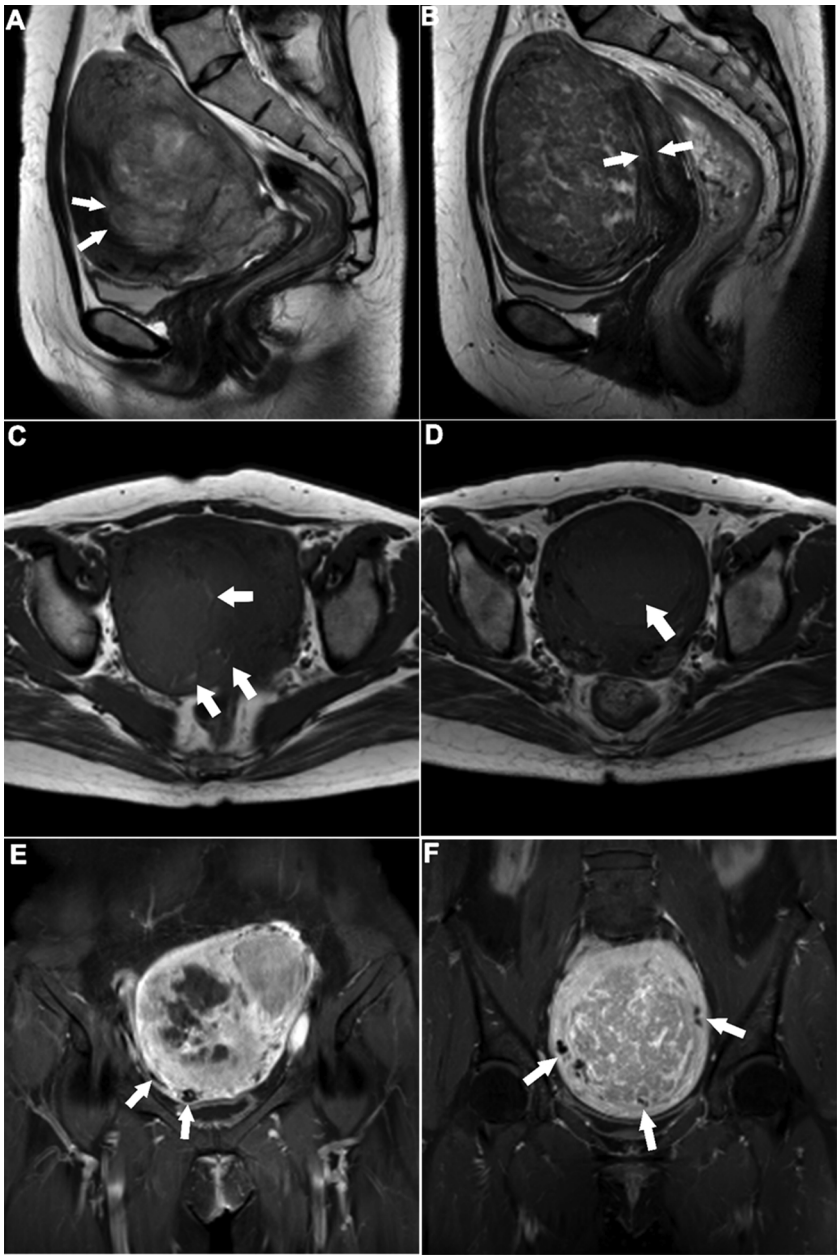

Fig. 2. Illustrations of the MRI feartures in uterine sarcoma (**A**, **C**, and **E**; images of a leiomyosarcoma in a 49-year-old woman) and leiomyoma (**B**, **D**, and **F**; images of a leiomyoma in a 48-year-old woman). **A** Sagittal T2-weighted images shows a large lobulated uterine mass with indistinct borderline and interrupted uterine endometrail cavity (white arrows). **B** Sagittal T2-weighted images shows a smooth large uterine mass with clear borderline and uninterrupted uterine endometrail cavity (white arrows). **C** and **D** T1-weighted images demonstrate intratumor hemorrahge in uterine sarcoma and leiomyoma (white arrows). **E** and **F** Coronal contrast-enhanced T1-wighted fat saturated images show the presence of pretumor increased vascularity (white arrows) and unenhanced necrosis.

sarcoma. The diagnostic efficacy achieved by radiomic model was comparable to those of experienced radiologists (AUC of 0.830 vs 0.752). According to results, radiologists had remarkable higher specificity (91.8%) than radiomic model (73.2%), but their sensitivity was rather low (58.6%). It illustrated radiologist tend to misdiagnose uterine sarcoma which may lead to poor prognosis. Partly because of the low occurrence risk of uterine sarcoma. Though the sample size is too small to make final conclusions about the value of the tool and its ability to help radiologists. It provides a new approach for the differentiation of uterine sarcoma and atypical leiomyoma in a non-invasive method. Training on many more cases will be required before we can decide its clinical value.

This work is also an attempt to demonstrate how radiomics can be employed to a very complex problem with very limited sample size. Since some image features are continuous in nature (e.g. necrosis can range from 0 to < 5% to > 50%), using an arbitrary binary index can significantly decreases data complexity and exaggerate categorization accuracies. So, we use mathematical ways to enrich quantitative data. Each volume was preprocessed using followed three extraction parameters before the extraction of radiomic features: (1) isotropic voxel size, (2) quantization of gray levels (quantization algorithm and number of gray levels). Considering the full set of Global features and higher-order texture features, a total of 1938 texture features were extracted from each VOI (Fig. 1) [24].

Our study had several limitations. First, it was a retrospective study, there was a selection bias for we only selected patients with preoperative MP-MRI and pathologic results. What's more, only one index lesion was chose for each patient. In cases where multiple atypical leiomyomas were presented in a hysterectomy specimen, this method also introduced a selection bias. Second, this study was partly based on the radiologist-selected imaging features. Although a good to excellent interobserver agreement has been achieved, it can be subjected to interobserver variability. Third, the number of patients included in this study was rather limited. A continuing problem for all computer aided learning will be defining a training set enough to determine a true normal. However, the low occurrence rate of uterine sarcoma determines that a large sample size will be very hard to achieve. Though collections and assessment of new cases is still ongoing by our group, a

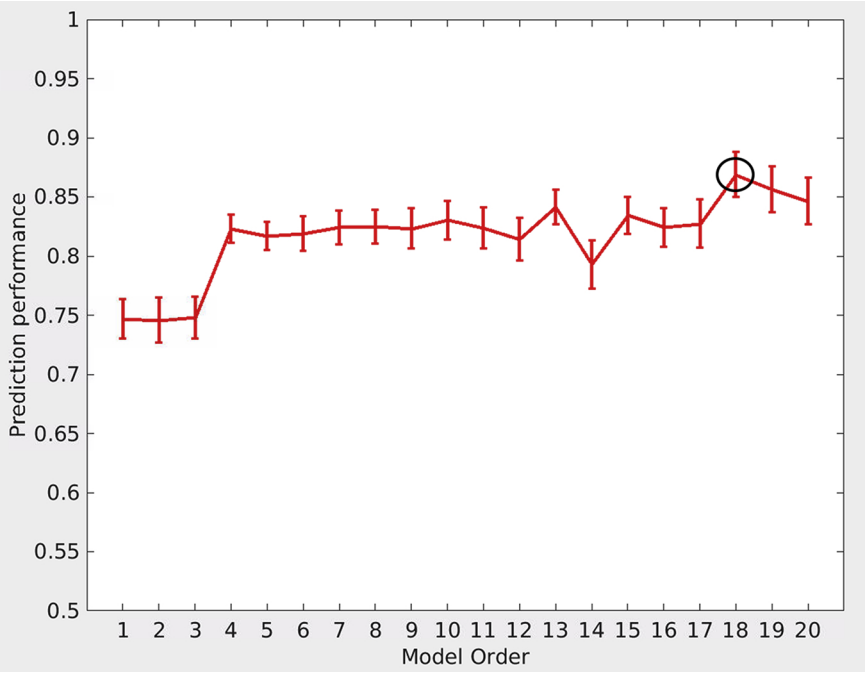

Fig. 3. Estimation of prediction performance of multivariable models constructed from apparent diffusion coefficient (ADC) maps using optimal degrees of freedom on texture extraction parameters, for model orders of 1-20. The optimal degrees of freedom were found in terms of maximum 0.632+ area under the receiver-operating characteristic curve (AUC) matrix, separately for each model order. Model 18 with 18 features yielded the highest AUC (black circle).

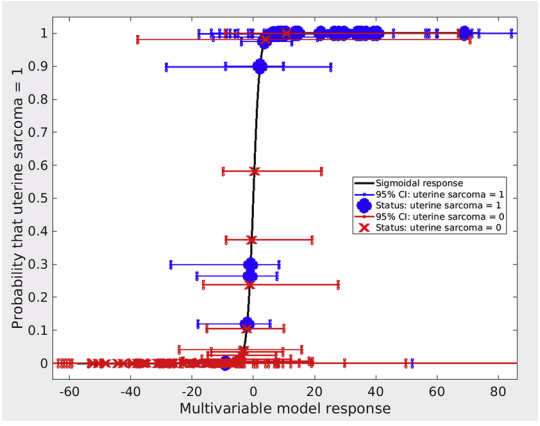

Fig. 4. Prediction performance of radiomic model. Probability of developing uterine sarcoma as a function of the response of the multivariable model proposed in this work, for all patients of the cohort. The dots represent patients who had uterine sarcoma and the crosses those who had uterine leiomyoma.

larger sample size with multiple compositions from different institutions and a distinct validation set are required. Fourth, we only assessed the radiomic features extracted from ADC maps in this study. Combination of T2WI and DCE images may improve the performance of radiomic analysis. Last, VOI was manually drawn which suffers from high interobserver variability and is time consuming. The optimum segmentation should be automatic, time efficient, and reproducible. Hopefully in future research, homogeneous evaluation criteria can be adopted to ensure the reproducibility of the radiomic studies.

In conclusion, our study demonstrates significant relationship between MRI features and pathological results. The preliminary attempt of multivariable texture model extracted from baseline ADC maps shows that radiomics can differentiate uterine sarcoma from atypical leiomyoma with comparable diagnostic efficacy to experienced radiologists. However, the sample size was too small, future training and validation are needed before deciding its clinical value.

Conflict of interest

We have received support from Interdisciplinary Clinical Research Project of Peking University First Hospital (2017CR21).

Appendix A. Supplementary data

Supplementary material related to this article can be found, in the online version, at doi:https://doi.org/10.1016/j.ejrad.2019.04.004.

References

[1] K. Pietzner, N. Buttmann-Schweiger, J. Sehouli, K. Kraywinkel, Incidence patterns and survival of Gynecological Sarcoma in Germany: analysis of population-based Cancer registry data on 1066 women, Int. J. Gynecol. Cancer 28 (1) (2018) 134–138.
[2] C. Wibmer, A. Leithner, N. Zielonke, M. Sperl, R. Windhager, Increasing incidence rates of soft tissue sarcomas? A population-based epidemiologic study and literature review, Ann. Oncol. 21 (5) (2010) 1106–1111.
[3] J. Zhang, J. Zhang, Y. Dai, L. Zhu, J. Lang, J. Leng, Clinical characteristics and management experience of unexpected uterine sarcoma after myomectomy, Int. J. Gynaecol. Obstet. 130 (2) (2015) 195–199.
[4] A. Gadducci, S. Cosio, A. Romanini, A.R. Genazzani, The management of patients with uterine sarcoma: a debated clinical challenge, Crit. Rev. Oncol. Hematol. 65 (2) (2008) 129–142.
[5] F. Amant, A. Coosemans, M. Debiec-Rychter, D. Timmerman, I. Vergote, Clinical management of uterine sarcomas, Lancet Oncol. 10 (12) (2009) 1188–1198.
[6] C. Owen, A.Y. Armstrong, Clinical management of leiomyoma, Obstet. Gynecol. Clin. North Am. 42 (1) (2015) 67–85.
[7] T.M. Picerno, M.N. Wasson, A.R. Gonzalez Rios, M.J. Zuber, N.P. Taylor, M.K. Hoffman, M.E. Borowsky, Morcellation and the incidence of occult uterine malignancy: a dual-institution review, Int. J. Gynecol. Cancer Off. J. Int. Gynecol. Cancer Soc. 26 (1) (2016) 149.
[8] Y. Lakhman, H. Veeraraghavan, J. Chaim, D. Feier, D.A. Goldman, C.S. Moskowitz, S. Nougaret, R.E. Sosa, H.A. Vargas, R.A. Soslow, N.R. Abu-Rustum, H. Hricak, E. Sala, Differentiation of uterine leiomyosarcoma from atypical leiomyoma: diagnostic accuracy of qualitative MR imaging features and feasibility of texture analysis, Eur. Radiol. 27 (7) (2017) 2903–2915.
[9] V. Tanos, K.E. Berry, Benign and malignant pathology of the uterus, best practice & research, Clin. Obstet. Gynaecol. 46 (2018) 12–30.
[10] T.H. Kim, J.W. Kim, S.Y. Kim, S.H. Kim, J.Y. Cho, What MRI features suspect malignant pure mesenchymal uterine tumors rather than uterine leiomyoma with cystic degeneration? J. Gynecol. Oncol. (2018).
[11] A. Sahdev, S.A. Sohaib, I. Jacobs, J.H. Shepherd, D.H. Oram, R.H. Reznek, MR

imaging of uterine sarcomas, AJR Am. J. Roentgenol. 177 (6) (2001) 1307–1311.
[12] Q. Bi, Z. Xiao, F. Lv, Y. Liu, C. Zou, Y. Shen, Utility of clinical parameters and multiparametric MRI as predictive factors for differentiating uterine sarcoma from atypical leiomyoma, Acad. Radiol. (2018).
[13] R. Aviram, Y. Ochshorn, O. Markovitch, A. Fishman, I. Cohen, M.M. Altaras, R. Tepper, Uterine sarcomas versus leiomyomas: gray-scale and Doppler sonographic findings, J. Clin. Ultrasound 33 (1) (2005) 10–13.
[14] T. Namimoto, Y. Yamashita, K. Awai, T. Nakaura, Y. Yanaga, T. Hirai, T. Saito, H. Katabuchi, Combined use of T2-weighted and diffusion-weighted 3-T MR imaging for differentiating uterine sarcomas from benign leiomyomas, Eur. Radiol. 19 (11) (2009) 2756–2764.
[15] K. Tamai, T. Koyama, T. Saga, N. Morisawa, K. Fujimoto, Y. Mikami, K. Togashi, The utility of diffusion-weighted MR imaging for differentiating uterine sarcomas from benign leiomyomas, Eur. Radiol. 18 (4) (2008) 723–730.
[16] R.J. Gillies, P.E. Kinahan, H. Hricak, Radiomics: images are more than pictures, they are data, Radiology 278 (2) (2016) 563–577.
[17] P. Lambin, R.T.H. Leijenaar, T.M. Deist, J. Peerlings, E.E.C. de Jong, J. van Timmeren, S. Sanduleanu, R. Larue, A.J.G. Even, A. Jochems, Y. van Wijk, H. Woodruff, J. van Soest, T. Lustberg, E. Roelofs, W. van Elmpt, A. Dekker, F.M. Mottaghy, J.E. Wildberger, S. Walsh, Radiomics: the bridge between medical imaging and personalized medicine, Nat. Rev. Clin. Oncol. 14 (12) (2017) 749–762.
[18] O. Gevaert, L.A. Mitchell, A.S. Achrol, J. Xu, S. Echegaray, G.K. Steinberg, S.H. Cheshier, S. Napel, G. Zaharchuk, S.K. Plevritis, Glioblastoma multiforme: exploratory radiogenomic analysis by using quantitative image features, Radiology 273 (1) (2014) 168–174.
[19] P. Prasanna, J. Patel, S. Partovi, A. Madabhushi, P. Tiwari, Radiomic features from the peritumoral brain parenchyma on treatment-naive multi-parametric MR imaging predict long versus short-term survival in glioblastoma multiforme: preliminary findings, Eur. Radiol. 27 (10) (2017) 4188–4197.
[20] C. Shen, Z. Liu, M. Guan, J. Song, Y. Lian, S. Wang, Z. Tang, D. Dong, L. Kong, M. Wang, D. Shi, J. Tian, 2D and 3D CT radiomics features prognostic performance comparison in non-small cell lung Cancer, Transl. Oncol. 10 (6) (2017) 886–894.
[21] H. Li, Y. Zhu, E.S. Burnside, K. Drukker, K.A. Hoadley, C. Fan, S.D. Conzen, G.J. Whitman, E.J. Sutton, J.M. Net, M. Ganott, E. Huang, E.A. Morris, C.M. Perou, Y. Ji, M.L. Giger, MR imaging radiomics signatures for predicting the risk of breast Cancer recurrence as given by research versions of Mamma Print, oncotype DX, and PAM50 gene assays, Radiology 281 (2) (2016) 382–391.
[22] A. Wibmer, H. Hricak, T. Gondo, K. Matsumoto, H. Veeraraghavan, D. Fehr, J. Zheng, D. Goldman, C. Moskowitz, S.W. Fine, V.E. Reuter, J. Eastham, E. Sala, H.A. Vargas, Haralick texture analysis of prostate MRI: utility for differentiating non-cancerous prostate from prostate cancer and differentiating prostate cancers with different Gleason scores, Eur. Radiol. 25 (10) (2015) 2840–2850.
[23] R.J. Kurman, M.L. Carcangiu, C.S. Herrington, R.H. Young, WHO Classification of Tumours of Female Reproductive Organs, (2014).
[24] M. Vallieres, C.R. Freeman, S.R. Skamene, I. El Naqa, A radiomics model from joint FDG-PET and MRI texture features for the prediction of lung metastases in soft-tissue sarcomas of the extremities, Phys. Med. Biol. 60 (14) (2015) 5471–5496.
[25] H. Zhou, M. Vallieres, H.X. Bai, C. Su, H. Tang, D. Oldridge, Z. Zhang, B. Xiao, W. Liao, Y. Tao, J. Zhou, P. Zhang, L. Yang, MRI features predict survival and molecular markers in diffuse lower-grade gliomas, Neurooncology 19 (6) (2017) 862–870.
[26] Y. Dong, Q. Feng, W. Yang, Z. Lu, C. Deng, L. Zhang, Z. Lian, J. Liu, X. Luo, S. Pei, X. Mo, W. Huang, C. Liang, B. Zhang, S. Zhang, Preoperative prediction of sentinel lymph node metastasis in breast cancer based on radiomics of T2-weighted fat-suppression and diffusion-weighted MRI, Eur. Radiol. 28 (2) (2018) 582–591.
[27] H. Brolmann, V. Tanos, G. Grimbizis, T. Ind, K. Philips, T. van den Bosch, S. Sawalhe, L. van den Haak, F.W. Jansen, J. Pijnenborg, F.A. Taran, S. Brucker, A. Wattiez, R. Campo, P. O'Donovan, R.L. de Wilde, European Society of Gynaecological Endoscopy steering committee on fibroid, options on fibroid morcellation: a literature review, Gynecol. Surg. 12 (1) (2015) 3–15.
[28] H. Brölmann, V. Tanos, G. Grimbizis, T. Ind, K. Philips, T.V.D. Bosch, S. Sawalhe, L.V.D. Haak, F.W. Jansen, J. Pijnenborg, Options on fibroid morcellation: a literature review, Gynecol. Surg. 12 (1) (2015) 3–15.
[29] V. Kumar, Y. Gu, S. Basu, A. Berglund, S.A. Eschrich, M.B. Schabath, K. Forster, H.J. Aerts, A. Dekker, D. Fenstermacher, D.B. Goldgof, L.O. Hall, P. Lambin, Y. Balagurunathan, R.A. Gatenby, R.J. Gillies, Radiomics: the process and the challenges, Magn. Reson. Imaging 30 (9) (2012) 1234–1248.
[30] A.R. Padhani, G. Liu, D.M. Koh, T.L. Chenevert, H.C. Thoeny, T. Takahara, A. Dzik-Jurasz, B.D. Ross, M. Van Cauteren, D. Collins, D.A. Hammoud, G.J. Rustin, B. Taouli, P.L. Choyke, Diffusion-weighted magnetic resonance imaging as a cancer biomarker: consensus and recommendations, Neoplasia 11 (2) (2009) 102–125.
[31] M. Takahashi, E. Kozawa, M. Tanisaka, K. Hasegawa, M. Yasuda, F. Sakai, Utility of histogram analysis of apparent diffusion coefficient maps obtained using 3.0T MRI for distinguishing uterine carcinosarcoma from endometrial carcinoma, J. Magn. Reson. Imaging 43 (6) (2016) 1301–1307.